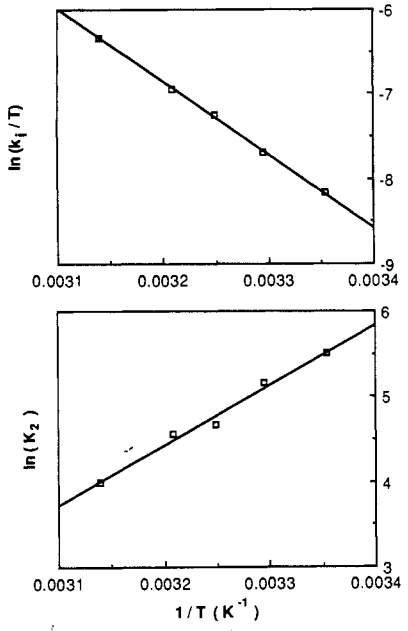

Figure 5. van't Hoff and Eyring plots illustrating the temperature dependences of K_2 and k_i (eq 2).

much slower isomerization rates observed ($t_{1/2} \geq 1$ h) indicate that [Pd(*C*-CA)(PPh_3)$_2$] rather than [Pd(*C*-CA)(PPh_3)(CH_3CN)] must be the predominant precursor to [Pd(π-CA)(PPh_3)$_2$] in the presence of excess PPh_3. Eyring and van't Hoff plots of ln (k_i/T) and ln K_2 vs $1/T$, respectively (Figure 5), yield the activation parameters of the isomerization step ($\Delta H^\ddagger = 17.1 \pm 0.3$ kcal/mol; $\Delta S^\ddagger = -6 \pm 2$ eu) and standard enthalpy/entropy changes corresponding to the uptake of a second PPh_3 ligand by [Pd(*C*-CA)(PPh_3)(CH_3CN)] ($\Delta H^\circ = -14.0 \pm 1.0$ kcal/mol; $\Delta S^\circ = -36 \pm 3$ eu).

The standard enthalpy and entropy changes related to K_2 are consistent with the bonding of a second PPh_3 ligand to Pd(II) at a sterically hindered coordination position cis to the first PPh_3 unit, which imposes a cone angle of 145°.[23] Indeed, an exceptionally negative $\Delta S^\circ(K_2)$ is primarily responsible for the unexpectedly small K_2 values that give rise to kinetic saturation behavior. In contrast, the activation barrier for linkage isomerization from [Pd(*C*-CA)(PPh_3)$_2$] to [Pd(π-CA)(PPh_3)$_2$] is predominantly enthalpic, as would be anticipated considering the stability of five-membered chelate rings containing one or more sp^3-hybridized carbon donor(s) to palladium(II).[24,25] Kinetic studies of tertiary phosphine substituent effects on the isomerization rate are currently being performed to elucidate the extent to which Lewis basicity of the P donor atoms trans to the carbanion leaving groups influences the activation barrier.[16] As measured by the product K_2k_i (2.1×10^1 M^{-1} s^{-1}, 25 °C; $\Delta H^\ddagger = 3.1$ kcal/mol, $\Delta S^\ddagger = -42$ eu), the overall substitutional reactivity of Pd(II) in reaction 1 is typical of that observed in related ligand-interchange processes.[26] Thus, these parameters closely resemble those for cyanide ligand exchange in $Pd(CN)_4^{2-}$ (k(24 °C) = 1.2×10^2 M^{-1} s^{-1}; $\Delta H^\ddagger$ = 4 kcal/mol, $\Delta S^\ddagger = -45$ eu).[27]

Linkage isomerization kinetic results reported here contrast strongly with mechanistic studies of β-elimination and reductive elimination reactions of coordinated alkyl groups in *cis*-PdL_2R_2 (L = tertiary phosphine) complexes.[28-30] Thus, reductive elimination of cis alkyl groups depends upon the prior *dissociation* of a phosphine ligand, such that the rate is strongly inhibited by excess phosphine in solution. However, treatment with 1,2-bis(diphenylphosphino)ethane induces the reduction of Pd(II) to Pd(0) in a palladacyclopentane complex, with concurrent evolution of *n*-butenes.[25]

Acknowledgment. Support of this research by the Robert A. Welch Foundation (Grant D-735) is gratefully acknowledged. We also wish to thank Dr. Jesse Yeh and Professor Jerry Mills for assistance in the acquisition of NMR spectra.

(23) Tolman, C. A. *Chem. Rev.* **1977**, *77*, 313.
(24) Newkome, G. R.; Kiefer, G. E.; Frere, Y. A.; Onishi, M.; Gupta, V. K.; Fronczek, F. R. *Organometallics* **1986**, *5*, 348.
(25) Diversi, P.; Ingrosso, G.; Lucherini, A. *J. Chem. Soc., Chem. Commun.* **1978**, 735.
(26) Atwood, J. D. *Inorganic and Organometallic Reaction Mechanisms*; Brooks-Cole: Monterey, CA, 1985.
(27) Pesek, J. J.; Mason, W. R. *Inorg. Chem.* **1983**, *22*, 2958.
(28) Ito, T.; Tsuchiya, H.; Yamamoto, A. *Bull. Chem. Soc. Jpn.* **1977**, *50*, 1319.
(29) Ozawa, F.; Ito, T.; Nakamura, Y.; Yamamoto, A. *Bull. Chem. Soc. Jpn.* **1981**, *54*, 1868.
(30) Milstein, D.; Stille, J. K. *J. Am. Chem.* Soc. **1979**, *101*, 4981.

Contribution from the Department of Chemistry, University of Houston, University Park, Houston, Texas 77004

Facile Rearrangement and Electron Transfer of 19-Electron Radicals from the Reduction of the Bischelated Manganese Carbonyl Cation $Mn(CO)_2[PPh_2(CH_2)_2PPh_2]_2^+$

D. J. Kuchynka and J. K. Kochi*

Received December 17, 1987

The cathodic reduction of the bischelated manganese carbonyl cation *trans*-$Mn(CO)_2(\eta^2\text{-DPPE})_2^+$ (I^+, where DPPE = $PPh_2(CH_2)_2PPh_2$) produces the metastable anion $Mn(CO)_2(\eta^2\text{-DPPE})(\eta^1\text{-DPPE})^-$ (II^-) via an overall 2e process at a Pt electrode in either tetrahydrofuran or acetonitrile solution. The unusual observation of a cathodic curve crossing and two isopotential points in the cyclic voltammogram of I^+ can be traced to an electron transfer with II^- to afford a pair of neutral radicals, i.e., the 19e $I^\bullet$ and the 17e $II^\bullet$. The former (which is also generated during the initial step in the reduction of I^+) is a metastable species and spontaneously extrudes an end of one DPPE ligand to afford the second radical $II^\bullet$ with the rate constant $k_r \approx 4 \times 10^6$ s^{-1}. The structures of the anionic and radical intermediates II^-, $II^\bullet$, and $I^\bullet$ are discussed in the context of their transient electrochemical behavior as well as their ^{31}P NMR and ESR spectra. The rather slow rate of electron transfer between I^+ and II^- is ascribed to steric effects in carbonylmanganese ions encumbered with a pair of DPPE ligands.

Introduction

Electrochemical methods can provide valuable mechanistic insight into the oxidation–reduction of various types of organometallic compounds, including metal carbonyls.[1,2] Among these, the reduction of diamagnetic carbonylmetal cations is especially intriguing since electron accession leads to electron-supersaturated 19e radicals that are highly labile and sensitive to ligand loss prior to dimerization.[2a,3] For example, the reduction of hexa-

(1) (a) Connelly, N. G.; Geiger, W. E. *Adv. Organomet. Chem.* **1984**, *23*, 18. (b) Carriedo, G. A.; Riera, V.; Connelly, N. G.; Raven, S. J. *J. Chem. Soc., Dalton Trans.* **1987**, 1769 and references therein.

(2) (a) Kuchynka, D. J.; Amatore, C.; Kochi, J. K. *Inorg. Chem.* **1986**, *25*, 4087. (b) Kochi, J. K. *J. Organomet. Chem.* **1986**, *300*, 139.

0020-1669/88/1327-2574$01.50/0

carbonylmanganese(I) yields the dimeric dimanganese decacarbonyl via CO loss, i.e.

$$Mn(CO)_6^+ \xrightarrow{+e^-} Mn(CO)_6^{\bullet} \xrightarrow{-CO} Mn(CO)_5^{\bullet}, \text{ etc.} \quad (1)$$

The monophosphine-substituted analogue undergoes competitive loss of either a CO or phosphine ligand, e.g.

$$Mn(CO)_5PPh_3^+ \xrightarrow{+e^-}$$

$$Mn(CO)_5PPh_3^{\bullet} \xrightarrow{40\%} CO + Mn(CO)_4PPh_3^{\bullet} \quad (2)$$

$$Mn(CO)_5PPh_3^{\bullet} \xrightarrow{60\%} PPh_3 + Mn(CO)_5^{\bullet} \quad (3)$$

In order to examine more closely the substitutional behavior of these 19e radicals, we have focused on the cathodic reduction of the bischelated cation[4]

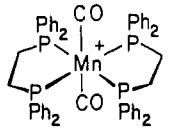

I^+

which is hereafter designated as *trans*-$Mn(CO)_2(\eta^2\text{-DPPE})^+$ or simply as I^+. The selection of this carbonylmanganese(I) cation was aimed at the optimum stabilization of the putative 19e radical, which should be favored by multiple phosphine substitution and difunctional ligands.[5]

Results and Discussion

I. Preparation of *trans*-$Mn(CO)_2(DPPE)_2^+$ Salts. The thermal disproportionation of dimanganese decacarbonyl by the added 1,2-bis(diphenylphosphino)ethane (DPPE) proceeded in refluxing benzene according to the stoichiometry in eq 4 (see Experimental Section). The mixed salt $I^+Mn(CO)_5^-$ was collected as yellow-

$$Mn_2(CO)_{10} + 2DPPE \rightarrow Mn(CO)_2(DPPE)_2^+Mn(CO)_5^- + 3CO \quad (4)$$

orange crystals in 73% yield, and it was readily analyzed by spectral subtraction of $Mn(CO)_5^-$ (ν_{CO} = 1865 and 1900 cm^{-1})[6] to reveal the single carbonyl IR band at 1897 cm^{-1}, previously identified with *trans*-$Mn(CO)_2(DPPE)_2^+$.[4,6] It was converted to the hexafluorophosphate salt by oxidative metathesis with $Cp_2Fe^+PF_6^-$ in acetonitrile to form $Mn_2(CO)_{10}$ as a byproduct, i.e.

$$Mn(CO)_2(DPPE)_2^+Mn(CO)_5^- + Cp_2Fe^+PF_6^- \rightarrow Mn(CO)_2(DPPE)_2^+PF_6^- + Cp_2Fe + {}^1/_2Mn_2(CO)_{10} \quad (5)$$

Somewhat analogously the perchlorate salt was prepared from $Mn(CO)_2(DPPE)^+Mn(CO)_5^-$ by the treatment of an acetonitrile solution with 1 equiv of silver perchlorate (see Experimental Section). The known chloride I^+Cl^- was prepared from the mixed salt obtained in eq 4 simply by dissolution in chloroform followed by the removal of $Mn_2(CO)_{10}$. Recrystallization from hexane–dichloromethane afforded golden yellow crystals. This halide salt and that prepared by the more conventional procedure,[4a] i.e.

$$Mn(CO)_5Br + 2DPPE \xrightarrow[\Delta]{MeOH} Mn(CO)_2(DPPE)_2^+Br^- \quad (6)$$

both showed a sharp singlet at δ 77.8 in the $^{31}P\{^1H\}$ NMR spectrum, even at −60 °C. The presence of a single phosphorus resonance coupled with the single carbonyl stretching band in the IR spectrum confirmed the previous assignment of the trans configuration of carbonyl ligands in I^+.[4,9]

II. Preparation and Spectral Identification of the Products and Intermediates in the Reduction of $Mn(CO)_2(DPPE)_2^+$. In order to facilitate the presentation of the electrochemical results, the structural assignments of the various carbonylmanganese intermediates and products will be presented separately as follows.

A. The anion $Mn(CO)_2(DPPE)_2^-$ (II^-) was produced during the preparative-scale electrolysis of $Mn(CO)_2(DPPE)_2^+PF_6^-$ in tetrahydrofuran solution containing 0.5 M tetra-*n*-butylammonium perchlorate (TBAP):

$$\underset{I^+}{Mn(CO)_2(DPPE)_2^+} + 2e^- \rightarrow \underset{II^-}{Mn(CO)_2(DPPE)_2^-} \quad (7)$$

The electroreduction was carried out in the dark and under an argon atmosphere (glovebox) at a constant potential of −2.0 V vs SCE. It resulted in the conversion of the initially yellow solution to a dark red one and an accompanying uptake of 1.95 equiv of charge for each mole of I^+ initially present. No evolution of CO was detected. The anion II^- was characterized in solution by a pair of carbonyl stretching bands at ν_{CO} = 1766 and 1710 cm^{-1} with equal intensity in the IR spectrum. The presence of two additional bands at higher energy (ν_{CO} = 1915 and 1856 cm^{-1}) was associated with the manganese hydride $HMn(CO)_2(DPPE)_2$ (III).[8] The relative amounts of II^- and III formed under these

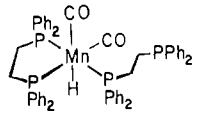

III

conditions were estimated to be roughly 40% and 60%, respectively. However, the anion II^- was the major product (~70%) when the electroreduction of $Mn(CO)_2(DPPE)_2^+$ was carried out in acetonitrile solution (see Experimental Section). All attempts to isolate the anion II^- as a crystalline salt for X-ray crystallography were unsuccessful owing to its spontaneous conversion to the hydride III (eq 8).[10] Indeed, this transformation was complete

$$\underset{II^-}{Mn(CO)_2(DPPE)_2^-} \xrightarrow{THF} \underset{III}{HMn(CO)_2(DPPE)_2}, \text{ etc.} \quad (8)$$

within 1 h in THF solution at room temperature, as indicated by the bleaching of the dark red color as well as the simultaneous disappearance of both IR bands at 1766 and 1710 cm^{-1} and concomitant growth of the bands at 1915 and 1856 cm^{-1}. The anion II^- was more persistent in acetonitrile solution, and the bleaching of the dark red color occurred slowly over a 12-h period. Moreover, the successive measurements of the IR spectra of this solution showed a steady decrease in the carbonyl bands of II^- at ν_{CO} = 1761 and 1706 cm^{-1} and growth of the corresponding bands of the hydride III at ν_{CO} = 1909 and 1844 cm^{-1}.[11] These results suggest that the anion II^- was initially formed as the primary product of the 2e reduction of the cationic $Mn(CO)_2(DPPE)_2^+$ according to eq 7 and was then subsequently transformed to the hydride III by proton transfer (eq 8) from either

(3) Narayanan, B. A.; Amatore, C.; Kochi, J. K. *Organometallics* **1987**, *6*, 129.
(4) (a) Stiddard, M. H. B.; Osborne, A. G. *J. Chem. Soc.* **1965**, 700. (b) Stiddard, M. H. B.; Snow, M. R. *J. Chem. Soc. A* **1966**, 777. (c) Sacco, A. *Gazz. Chim. Ital.* **1963**, *93*, 698.
(5) See, e.g.: Richmond, M. G.; Kochi, J. K. *Inorg. Chem.* **1986**, *25*, 656; *Organometallics* **1987**, *6*, 254.
(6) The reaction analogous to that in eq 4 was erroneously reported to give the bisbridged dinuclear carbonyl $Mn_2(CO)_6(\eta^2\text{-DPPE})_2$, which was misassigned owing to the overlay of the carbonyl bands of $Mn(CO)_5^-$ (ν_{CO} = 1899 and 1865 cm^{-1} as described by: King, R. B.; Stone, F. G. A. *Inorg. Synth.* **1963**, *3*, 198. Wrighton, M. S.; Faltynek, R. A. *J. Am. Chem. Soc.* **1978**, *100*, 2701) and those of $Mn(CO)_2(DPPE)_2^+$ (ν_{CO} = 1897 cm^{-1}).[4]
(7) Reimann, R. H.; Singleton, E. *J. Organomet. Chem.* **1972**, *38*, 113.
(8) Kuchynka, D. J.; Kochi, J. K., to be submitted for publication.
(9) Bond, A. M.; Snow, M. R.; Wimmer, F. L. *Inorg. Chem.* **1974**, *13*, 1617.
(10) Reaction (eq 8) not balanced owing to the ambiguity of the proton source.
(11) Note the shifts of the carbonyl bands in the more polar acetonitrile. For solvent effects on ion pairing, see: (a) Kao, S. C.; Darensbourg, M. Y.; Schenk, W. *Organometallics* **1984**, *3*, 871. (b) Darensbourg, D. J.; Darensbourg, M. Y. *Inorg. Chim. Acta* **1971**, *5*, 247. (c) Darensbourg, M. Y.; Jiminez, P.; Sackett, J. R. *J. Organomet. Chem.* **1980**, *202*, C68. (d) Darensbourg, M. Y.; Hanckel, J. M. *J. Organomet. Chem.* **1981**, *217*, C9. (e) Drew, D.; Darensbourg, D. J.; Darensbourg, M. Y. *J. Organomet. Chem.* **1975**, *85*, 73.

the supporting electrolyte or the solvent.[12-15] The hydride III was the ultimate, stable product of reduction, and it could be converted back to the basic anion II^- only by deprotonation with strong bases such as *n*-butyllithium at −45 °C (see Experimental Section).

The anion II^- is structurally akin to the anion IV^- obtained from the 2e reduction of the tetrakis(trimethyl phosphite) analogue $Mn(CO)_2[P(OMe)_3]_4^+$ by the same procedure used in eq 7 (see Experimental Section). However, it is important to note that

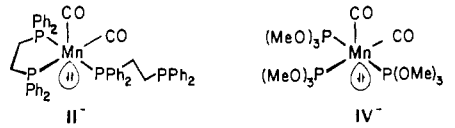

II^- IV^-

the initially formed 6-coordinate anion $Mn(CO)_2[P(OMe)_3]_4^-$ as a 20e species was unstable and resulted in the loss of a $P(OMe)_3$ ligand during the reduction, i.e.

$$Mn(CO)_2[P(OMe)_3]_4^+ \xrightarrow{2e^-} \underset{IV^-}{Mn(CO)_2[P(OMe)_3]_3^-} + P(OMe)_3$$

Thus the pair of carbonyl stretching bands at ν_{CO} = 1821 and 1757 cm^{-1} observed in the IR spectrum of the catholyte relates to the tris-substituted anion $Mn(CO)_2[P(OMe)_3]_3^-$ (IV^-), which is identical with that prepared earlier by a standard sodium amalgam reduction of the bromo tris(phosphite) complex *cis*-$Mn(CO)_2[P(OMe)_3]_3Br$, i.e.[16,19,20]

$$Mn(CO)_2[P(OMe)_3]_3Br \xrightarrow{Na(Hg)} \underset{IV^-}{Mn(CO)_2[P(OMe)_3]_3^-} + Br^- \quad (9)$$

Correspondingly, we infer the structure of the chelated anion II^- to be $Mn(CO)_2(\eta^2\text{-DPPE})(\eta^1\text{-DPPE})^-$, i.e., with an end of one bis(phosphine) ligand pendant.[21] The latter is supported by (a) the similarity of the anion II^- to the monodentate analogue $Mn(CO)_2(DPPE)PPhMe_2^-$,[24] (b) the ready replacement of the pendant, monodentate DPPE ligand in the anion II^- to the known anion $Mn(CO)_3(DPPE)^-$ (V^-)[17] immediately upon its exposure to an atmosphere of CO, i.e.[26]

$$II^- + CO \xrightarrow{\text{very fast}} \underset{V^-}{Mn(CO)_3(DPPE)^-} + DPPE \quad (10)$$

and (c) the protonation of II^- to the hydridomanganese complex III,[27] i.e.

$$II^- + CH_3CO_2H \rightarrow \underset{III}{HMn(CO)_2(DPPE)_2} + OAc^-$$

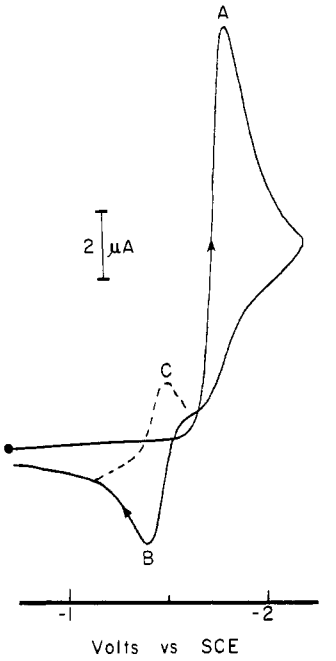

Figure 1. Initial negative-scan cyclic voltammogram of 5 × 10^{-3} M $Mn(CO)_2(DPPE)_2^+PF_6^-$ in THF containing 0.3 M TBAP at v = 500 mV s^{-1}.

B. The radical $Mn(CO)_2(DPPE)_2^\bullet$ exists in two forms, $I^\bullet$ and $II^\bullet$, which are structurally related to the cationic precursor I^+ and anionic precursor II^-, respectively. As such, the 6-coordinate $Mn(CO)_2(\eta^2\text{-DPPE})_2^\bullet$ and the 5-coordinate $Mn(CO)_2(\eta^2\text{-DPPE})(\eta^1\text{-DPPE})^\bullet$ represent 19e and 17e radicals, respectively. Furthermore, they are also related conceptually by an intramolecular rearrangement resulting from the making or breaking of a manganese–phosphorus bond to a chelating bisphosphine ligand.[28] However, radicals $I^\bullet$ and $II^\bullet$ were not interconvertible. Thus, Figure 1 shows the negative-scan cyclic voltammogram (CV) of $Mn(CO)_2(\eta^2\text{-DPPE})_2^+$, in which the initial cathodic wave A

(12) (a) M'Halla, F.; Pinson, J.; Saveant, J. M. *J. Am. Chem. Soc.* **1980**, *102*, 4120. (b) Tyler, D. R.; Goldman, A. S. *J. Organomet. Chem.* **1986**, *311*, 349.
(13) (a) Dessy, R. E.; Pohl, R. L.; King, R. B. *J. Am. Chem. Soc.* **1966**, *88*, 5121. (b) Dessy, R. E.; Weissman, P. M. *J. Am. Chem. Soc.* **1966**, *88*, 5124. (c) Dessy, R. E.; Weissman, P. M. *J. Am. Chem. Soc.* **1966**, *88*, 5129.
(14) Davies, J. A.; Eagle, C. T. *Organometallics* **1986**, *5*, 2149.
(15) This formulation is also supported by the absence of the cathodic wave of $HMn(CO)_2(DPPE)_2$ at E_p = −2.60 V in the initial negative-scan CV (0.5 V s^{-1}) of I^+. Thus, III is not a direct product of the reduction of I^+ on the CV time scale. Further evidence accrues from the CV of I^+ in the presence of as little as 2 equiv of acetic acid. An initial negative scan shows the reduction of I^+ at −1.84 V, and continued scanning to −2.9 V shows a very large reduction wave at −2.60 V. Scan reversal at −2.10 V reveals the complete absence of all the anodic waves associated with the I^+ reduction.
(16) For the 2e reduction of $BrMn(CO)_{5-x}L_x$ to the corresponding anions $Mn(CO)_{5-x}L_x$, see ref 17 and 18.
(17) Kuchynka, D. J.; Amatore, C. A.; Kochi, J. K. *J. Organomet. Chem.* **1987**, *328*, 133.
(18) (a) Hieber, W.; Hofler, M.; Muschi, J. *Chem. Ber.* **1965**, *98*, 311. (b) Hieber, W.; Faulhaber, G.; Theubert, F. *Z. Anorg. Allg. Chem.* **1962**, *314*, 125. (c) Onaka, S.; Yoshikawa, Y.; Yamatera, H. *J. Organomet. Chem.* **1978**, *157*, 187.
(19) Berke, H.; Weiler, G. *Z. Naturforsch., B.: Anorg. Chem., Org. Chem.* **1984**, *39B*, 431.
(20) Treichel, P. M.; Benedict, J. J. *J. Organomet. Chem.* **1969**, *17*, 37. The IR bands reported at ν_{CO} = 1954 and 1890 cm^{-1} result from oxidation of IV^- by $CHCl_3$, and they probably are due to $HMn(CO)_2[P(OMe)_3]_3$.[19]
(21) Since there is an increasing trend away from the trigonal-bipyramidal configuration of $Mn(CO)_5^-$ with phosphine substitution,[22] we formulate the sterically encumbered $Mn(CO)_2P_3^-$ as favoring the square-pyramidal configuration shown above. Furthermore, theoretical studies[23] indicate only a small energy difference between these configurations in $Mn(CO)_5^-$ that could be easily inverted by the added electronic, steric, and chelation effects induced by DPPE ligands. Note that the 17e radical prefers the square-pyramidal configuration (vide infra)[40] and that the electron transfer $II^- \rightleftharpoons II^\bullet$ is chemically as well as electrochemically reversible—indicative of a small structural difference between the anion and the radical.
(22) (a) Frenz, B. A.; Ibers, J. A. *Inorg. Chem.* **1972**, *11*, 1109. (b) Davis, R. E.; Riley, P. E. *Inorg. Chem.* **1980**, *19*, 159.
(23) (a) Hoffmann, R.; Rossi, A. R. *Inorg. Chem.* **1975**, *14*, 365. Elian, M.; Hoffmann, R. *Inorg. Chem.* **1975**, *14*, 1058. (b) Pensak, D. A.; McKinney, R. J. *Inorg. Chem.* **1979**, *18*, 3407.
(24) Prepared from the 2e reduction of $BrMn(CO)_2(DPPE)(PPhMe_2)$.[25]
(25) Compare: Riemann, R. H.; Singleton, E. *J. Chem. Soc., Dalton Trans.* **1973**, 841.
(26) For details, see the Experimental Section.
(27) The structure of III with cis carbonyls is elaborated separately.[8]
(28) For 17e and 19e radicals, see discussion in ref 2. See also: (a) Kidd, D. R.; Brown, T. L. *J. Am. Chem. Soc.* **1978**, *100*, 4095. (b) Byers, B. H.; Brown, T. L. *J. Am. Chem. Soc.* **1977**, *99*, 2527. (c) Hoffman, N. W.; Brown, T. L. *Inorg. Chem.* **1978**, *17*, 613. (d) Absi-Halabi, M.; Brown, T. L. *J. Am. Chem. Soc.* **1977**, *99*, 2982. (e) Fox, A.; Malito, J.; Poe, A. J. *J. Chem. Soc., Chem. Commun.* **1981**, 1052. (f) McCullen, S. B.; Walker, H. W.; Brown, T. L. *J. Am. Chem. Soc.* **1982**, *104*, 4007. (g) Shi, Q.-Z.; Richmond, T. G.; Trogler, W. C.; Basolo, F. *J. Am. Chem. Soc.* **1982**, *104*, 4032. (h) Herrington, T. R.; Brown, T. L. *J. Am. Chem. Soc.* **1985**, *107*, 5700. (i) Doxsee, K. M.; Grubbs, R. H.; Anson, F. C. *J. Am. Chem. Soc.* **1984**, *106*, 7819. (j) Turaki, N. N.; Huggins, J. M. *Organometallics* **1986**, *5*, 1703 and relevant references therein. (k) Goldman, A. S.; Tyler, D. R. *Comments Inorg. Chem.* **1986**, *5*, 215.

Table I. Sweep-Rate Dependence of the Peak Separation in the B/C Coupled Wave[a]

v, V s^{-1}	E_p^a, V[b]	ΔE_p, V[c]	i_p^a, μA[d]	i_p^c/i_p^a
0.02	−1.435	0.067	2.31	0.97
0.05	−1.431	0.077	3.56	0.97
0.10	−1.429	0.080	4.94	0.96
0.20	−1.424	0.087	6.75	0.96
0.50	−1.416	0.100	10.0	0.97

[a] From 1×10^{-2} M $Mn(CO)_2(DPPE)^+PF_6^-$ in THF containing 0.3 M TBAP. Potential measured relative to SCE. [b] Anodic peak potential. [c] $\Delta E_p = E_p^a - E_p^c$. [d] Anodic peak current.

($E_p^c = -1.84$ V at 0.5 V s^{-1}) corresponded to a 2e reduction of I^+, as calibrated with a ferrocene standard.[29] This initial 2e cathodic wave remained irreversible even at CV scan rates exceeding 100 000 V s^{-1} that were achieved with a Pt microelectrode.[30] Such an electrochemical behavior of I^+ is indicative of an ECE process as outlined in Scheme I,[31,32] where the rate of

Scheme I

$$I^+ \xrightarrow{e^-} I^\bullet \quad (11)$$

$$I^\bullet \xrightarrow[0]{k_r} II^\bullet \quad (12)$$

$$II^\bullet \rightleftharpoons^{e^-} II^- \quad (13)$$

radical rearrangement has a minimum value of $k_2 \approx 4 \times 10^6$ s^{-1}.[31a,33] The formation of the anion II^- is shown in the cyclic voltammogram (Figure 1) by the presence of the anodic wave B on the return scan, which represents the oxidation of the anion II^- to the radical $II^\bullet$. As such, the anodic wave B with $E_p^a = -1.39$ V is the same as that in a cyclic voltammogram obtained from the initial positive scan of the anion II^-, as prepared in eq 7. The associated reduction of the radical $II^\bullet$ back to the anion is represented by the cathodic wave C, and it is indicated in Figure 1 by the dashed curve. We emphasize that wave C occurs at a peak potential of $E_p^c = -1.52$ V, which is substantially more positive than $E_p^c = -1.84$ V, for the reduction of the cationic I^+. As a result, all three steps in Scheme I are included as the single 2e wave A in Figure 1.[34] The chemically reversible nature of the 1e oxidation of II^- to the 17e radical $II^\bullet$ with $E_{1/2} = -1.45$ V was established by the ratio of the anodic (B) and cathodic (C) peak currents $i_p^c/i_p^a = 1$, i.e.

$$Mn(CO)_2(\eta^2\text{-DPPE})(\eta^1\text{-DPPE})^- \underset{II^-}{\rightleftharpoons} Mn(CO)_2(\eta^2\text{-DPPE})(\eta^1\text{-DPPE})^\bullet + e^- \quad (14)$$
$$II^\bullet$$

The CV wave analysis for the oxidation of II^- and the reduction of $II^\bullet$ in Figure 1 indicated that the B/C coupled wave was quasi-reversible—the shape and peak separation being controlled by diffusion and the kinetics of electron transfer.[35,36] Indeed, the rather slow heterogeneous rate constant for electron transfer in eq 13 was evaluated as $k_s = 8 \times 10^{-3}$ cm s^{-1} with $\alpha = 0.4$ from the plot of the peak separation ($\Delta E_p = E_p^a - E_p^c$) as a function of the CV scan rate listed in Table I. Nonetheless, the chemically reversible $II^-/II^\bullet$ couple is consistent with an electron-transfer process that occurs with only minor structural changes in the anion and radical.[37]

The ESR spectrum shown in Figure 2A was obtained from the anodic oxidation of the anion II^- at −1.4 V in acetonitrile containing 0.1 M tetra-*n*-butylammonium tetrafluoroborate. We were unable to further resolve the rather broadened spectrum at $\langle g \rangle = 2.025$ with peak-to-peak line widths of ~15 G. The latter together with the slightly irregular pattern of line intensities made an unambiguous structural assignment somewhat difficult. Nonetheless, the principal features of the spectrum were assigned to a pair of equivalent phosphorus nuclei with $a_P \cong 20$ G and a third phosphorus nucleus with $a_P = 42$ G. The small ^{55}Mn hfs of $a_{Mn} \cong 9$ G and the fourth ^{31}P hfs of $a_P \cong 17$ G were deduced from the computer simulation shown in Figure 2B (see Experimental Section for details). The ESR parameters for $II^\bullet$ are consistent with those of analogous 17e radicals examined earlier by Brown and co-workers,[38] viz., $Mn(CO)_3(PBu_3)_2^\bullet$ with $\langle g \rangle = 2.030$, $a_{Mn} = 7$ G, and $a_P = 21$ G and $Mn(CO)_3[P(OEt)_3]_2^\bullet$ with $\langle g \rangle = 2.031$, $a_{Mn} = 14$ G, and $a_P = 42$ G. Indeed, the square-pyramidal configuration of these Mn(0) radicals together with the ^{31}P hfs pattern for the three phosphine ligands[39] in *mer*-$Cr(CO)_3(PMe_2Ph)_3^{\bullet+}$ leads to an analogous structure for $II^\bullet$:[40]

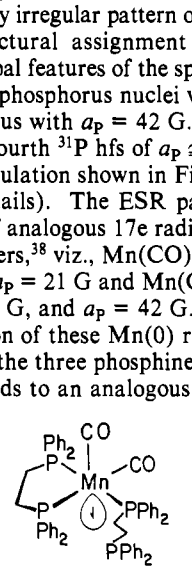

$II^\bullet$

In this structure, the incipient interaction of the pendant phosphine center with the singly occupied orbital leads to the smallest ^{31}P hfs (17 G), and this interaction is reminiscent of the partial

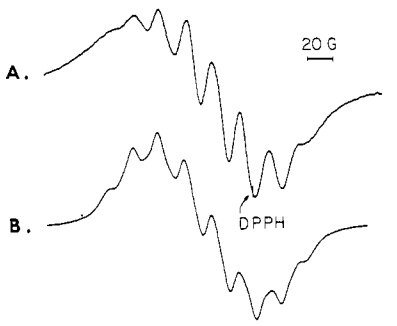

Figure 2. (A) Experimental ESR spectrum obtained from the anodic oxidation of II^- at −1.4 V in acetonitrile containing 0.3 M TBAP. (B) Computer-simulated ESR spectrum based on the parameters described in the text.

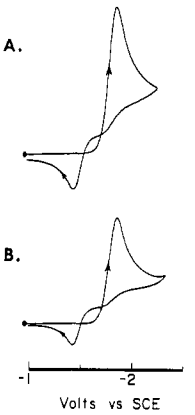

Figure 3. Curve crossing in the cyclic voltammetry of $Mn(CO)_2(DPPE)_2^+$ at sweep rates of (A) 200 mV s^{-1} and (B) 50 mV s^{-1}.

(29) Gagne, R. R.; Koval, C. A.; Lisensky, G. C. *Inorg. Chem.* **1980**, *19*, 2854.
(30) See: Howell, J. O.; Goncalves, J. M.; Amatore, C.; Klasinc, L.; Wightman, R. M.; Kochi, J. K. *J. Am. Chem. Soc.* **1984**, *106*, 3968.
(31) (a) Nicholson, R. S.; Shain, I. *Anal. Chem.* **1965**, *37*, 178. (b) Saveant, J. M. *Electrochim. Acta* **1967**, *12*, 753.
(32) Gaudiello, J. G.; Wright, T. C.; Jones, R. A.; Bard, A. J. *J. Am. Chem. Soc.* **1985**, *107*, 888.
(33) Nicholson, R. S.; Shain, I. *Anal. Chem.* **1964**, *36*, 706.
(34) Calibration of CV wave A relative to the reversible anodic curve of I^+ at 0.98 V corresponds to the uptake of 1.6e.
(35) Bard, A. J.; Faulkner, L. R. In *Electrochemical Methods*; Wiley: New York, 1980; p 181.
(36) Nadjo, L.; Saveant, J. M. *J. Electroanal. Chem. Interfacial Electrochem.* **1973**, *48*, 113.
(37) For the peak-to-peak separation of $\Delta E_p \approx 100$ mV at 500 mV s^{-1}.
(38) Kidd, D. R.; Cheng, C. P.; Brown, T. L. *J. Am. Chem. Soc.* **1978**, *100*, 4103.
(39) Bond, A. M.; Carr, S. W.; Colton, R. *Inorg. Chem.* **1984**, *23*, 2343.
(40) The 17e $Mn(CO)_5^\bullet$ has a square-pyramidal structure in argon and CO matrices: Symons, M. C. R.; Sweany, R. L. *Organometallics* **1982**, *1*, 834. Church, S. P.; Poliakoff, R. L.; Timney, J. A.; Turner, J. J. *J. Am. Chem. Soc.* **1981**, *103*, 7515. Theoretical studies also indicate the square-pyramidal configuration to be favored.[23]

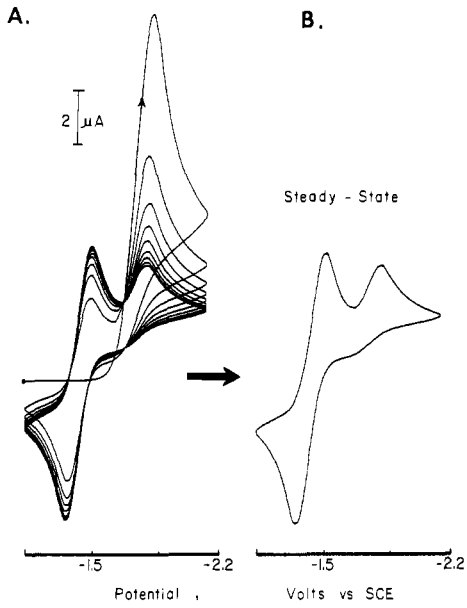

Figure 4. (A) Repetitive (10-cycle) cyclic voltammogram of 5×10^{-3} M $Mn(CO)_2(DPPE)_2^+PF_6^-$ in THF containing 0.3 M TBAP at $v = 500$ mV s^{-1}. (B) Steady-state CV after 25 cycles.

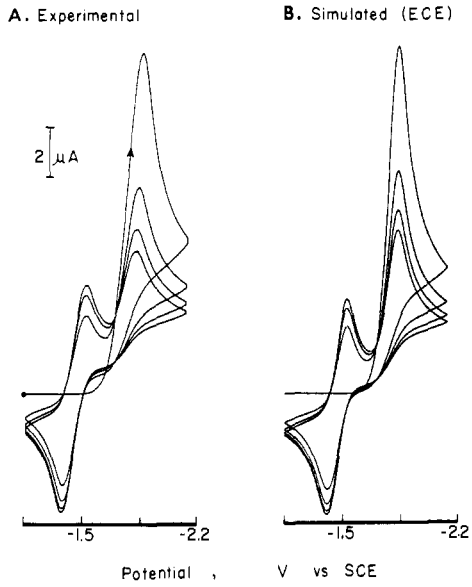

Figure 5. (A) Initial negative scan (4-cycle) cyclic voltammogram of 5×10^{-3} M $I^+PF_6^-$ with 0.3 M TBAP at $v = 500$ mV s^{-1}. (B) Computer-simulated CV according to ECE mechanism in Scheme I.

bonding in *mer*-$Mo(CO)_3(\eta^2\text{-DPPE})(\eta^1\text{-DPPE})^{\bullet+}$, as described by Bond and co-workers.[41]

III. Transient Electrochemical Behavior of $Mn(CO)_2(DPPE)_2^+$. The cyclic voltammogram in Figure 1 provides unusual insight into the mechanistic pathway by which the chelated cation I^+ was reduced to the anion II^- according to the stoichiometry in eq 7. Most unusual is the *curve crossing* at $E \approx -1.6$ V, in which the current on the return scan is actually more *cathodic* than that on the initial negative scan. The magnitude of the curve crossing was more pronounced at a slower scan rate, as shown by a comparison of the cyclic voltammogram in Figure 1 ($v = 500$ mV s^{-1}) with those in Figure 3A ($v = 200$ mV s^{-1}) and Figure 3B ($v = 50$ mV s^{-1}). Interestingly, when the cyclic voltammetry was repeatedly cycled between −1.1 and −2.2 V (see Figure 4A), it attained the steady-state cyclic voltammogram shown in Figure 4B. Thus after ~15 cycles the CV wave A for $Mn(CO)_2(DPPE)_2^+$ was reduced to one-fourth of its original peak current and the B/C wave of the $II^-/II^{\bullet}$ couple was dominant. Two isopotential points (IPP; akin to isosbestic points in spectroscopy[42]) indicated that one electroactive species was quantitatively converted to another, the sum of the reactant and product concentrations thus remaining constant. (As we will show later, the positions of these IPPs are extremely sensitive to the rate of disproportionation between I^+ and its reduced product (II^-).)

IV. Mechanism of the Cathodic Reduction of $Mn(CO)_2(DPPE)_2^+$ by CV Simulation. The ECE sequence depicted in Scheme I (eq 11–13) represents the most economical pathway for the reduction of the cationic $Mn(CO)_2(DPPE)_2^+$ to the anion II^-. The essential correctness of this formulation is illustrated in Figure 5 by the computer simulations (Figure 5B) of the experimental cyclic voltammograms (Figure 5A) over a sequence of four repetitive cycles. The CV simulations were carried out by using Feldberg's finite difference (digital) method[43,44] with the following optimized electrochemical parameters. The heterogeneous rate constant $k_1^s = 5.0 \times 10^{-3}$ cm s^{-1} for wave A (see Figure 1) and the standard reduction potential $E^\circ_1 = -1.76$ V were set to yield $E_p^c = -1.84$ V with the experimentally determined transfer coefficient $\alpha = 0.4$ (vide supra). The parameters for the chemically reversible $II^-/II^{\bullet}$ redox couple for the B/C wave in Figure 1 were chosen to give $E^\circ_2 = -1.45$ V [the experimentally observed $E_{1/2}$ value (vide supra)[45]] and the peak separation $\Delta E_p = 100$ mV at the scan rate $v = 500$ mV s^{-1}. The best results were obtained with the heterogeneous rate constant for eq 13 as $k_2^s = 1.1 \times 10^{-2}$ cm s^{-1} and the transfer coefficient $\alpha = 0.4$, both of which compare favorably with the experimentally determined values $k_2^s = 8 \times 10^{-3}$ cm s^{-1} and $\alpha = 0.4$. The diffusion coefficients taken from related carbonylmanganese anions were set as 5×10^{-6} cm^2 s^{-1}.[17] The rate constant for rearrangement in eq 12 was $k_r = 4 \times 10^6$ s^{-1} since it was the minimum value estimated from the irreversible cyclic voltammogram at $v = 10^5$ V s^{-1} (vide supra). However, even a rate constant of this magnitude was not completely necessary since the initial cathodic current became independent of the value of k_r on the time scale of the CV experiment (estimated to be ~10^2 s^{-1} at $v = 500$ mV s^{-1}). Since it did have a minor effect on the position of the CV wave, the value of E°_1 was adjusted to give the experimental value $E_p^c = -1.84$ (vide supra).

Although the general features of the computer-simulated cyclic voltammograms in Figure 5 resembled the experimental ones, a closer scrutiny revealed three important discrepancies.

(a) A pair of IPPs were observed in the simulated CV. However, they occurred at the same potential, which was not the situation in the experimental CV (vide supra).

(b) No curve crossing was brought out in the simulated cyclic voltammograms.

(c) The cathodic peak current for the reduction of I^+ on the fourth cycle was substantially larger than that observed experimentally.

When they were all taken together, these discrepancies pointed toward the necessity of including an additional factor that would reduce the concentration of I^+ faster on successive scans and concomitantly produce an electroactive species reducible at a more positive potential than for I^+. A disproportionation process between I^+ and its reduced product II^- that gave rise to the pair of radicals $I^{\bullet}$ and $II^{\bullet}$ could produce the desired effect,[46] i.e.

$$\underset{I^+}{Mn(CO)_2(DPPE)_2^+} + \underset{II^-}{Mn(CO)_2(DPPE)(\eta^1\text{-DPPE})^-} \rightleftharpoons \underset{19e}{I^{\bullet}} + \underset{17e}{II^{\bullet}} \quad (15)$$

(41) Bond, A. M.; Colton, R.; McGregor, K. *Inorg. Chem.* **1986**, *25*, 2378.
(42) (a) Untereker, D. F.; Bruckenstein, S. *Anal. Chem.* **1972**, *44*, 1009. (b) Untereker, D. F.; Bruckenstein, S. *J. Electroanal. Chem. Interfacial Electrochem.* **1974**, *57*, 77.
(43) (a) Feldberg, S. W. In *Electroanalytical Chemistry*; Bard, A. J., Ed.; Dekker: New York, 1969; Vol. 3, p 199. (b) Feldberg, S. W. In *Computer Applications in Analytical Chemistry*; Mark, H. B., Ed.; Dekker: New York, 1972; p 185.
(44) (a) Hershberger, J. W.; Klingler, R. J.; Kochi, J. K. *J. Am. Chem. Soc.* **1983**, *105*, 61. (b) Bockman, T. M.; Kochi, J. K. *J. Am. Chem. Soc.* **1987**, *109*, 7725.
(45) For E° values from CV data, see ref 30.

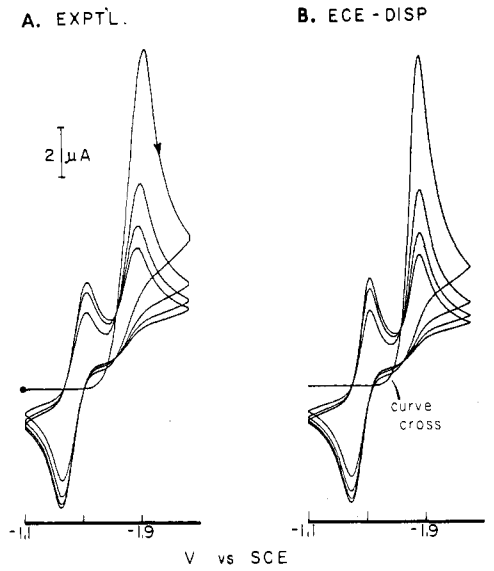

Figure 6. (A) Repetitive 4-cycle CV of $Mn(CO)_2(DPPE)_2^+$ as in Figure 5A. (B) Computer simulated CV's based on ECE-DISP mechanism with the inclusion of eq 16.

Owing to the rapid conversion of the 19e radical to II•, this process was approximated as

$$I^+ + II^- \underset{k_d}{\overset{k_{et}}{\rightleftharpoons}} 2II^\bullet \qquad (16)$$

where k_{et} is the rate constant for electron transfer in the ion pair and k_d is the rate constant for radical disproportionation. Since the radical II• is persistent on the CV time scale and unable to dimerize,[47,48] any reaction such as eq 16 which produces a steady-state concentration of II• at potentials that are negative of E°_2 will result in a continuous flow of cathodic current and, hence, curve crossing. In order to establish this conclusion, the series of cyclic voltammograms in Figure 5 were simulated again with the inclusion of the disproportionation process. Figure 6 shows the computer-simulated voltammogram constructed from the ECE-DISP model based on eq 11–13 and 16. Excellent agreement with the experimental CV was obtained with the same electrochemical parameters employed in Figure 5B (vide supra), together with $k_{et} = 35\ M^{-1}\ s^{-1}$ and $k_d = 5.3\ M^{-1}\ s^{-1}$. Furthermore, the isopotential points at −1.71 and −1.73 V were in excellent agreement with the experimental IPPs. Most importantly, the amount of the cathodic curve-crossing current was clearly seen to match the experimental phenomenon.[49] The variations in the value of k_{et} were mirrored in the cathodic current in the curve-crossing region as expected. However, more diagnostic was the behavior of the first scan (of the four-cycle simulated voltammograms), which did not pass through an IPP at −1.70 V when k_{et} was increased, clearly at variance with experiment (see Figure 6A). This effect was not an artifact of the digital simulation method, and it had also been observed in systems that undergo faster disproportionation.[32]

V. Comments on the Driving Force and Rates of Electron Transfer in Ion-Pair Annihilation. The standard potentials for the reduction of I^+ and the oxidation of II^-, as obtained from the CV simulation, indicate that the driving force for the electron transfer in eq 16 is −7 kcal mol^{-1}.[50] However, this estimate is based on the assumption that the rapid ligand expulsion from the initially formed 19e radical I• to afford II• is tantamount to the electron transfer in eq 16 and drives the reaction to the right. If the rearrangement is assumed to be reversible with an equilibrium constant of $K = 4 \times 10^6$, the standard potential of I^+ is estimated to be $E^\circ_2 = -1.37$ V and the driving force for electron transfer in eq 15 is ≅2 kcal mol^{-1}.[51] In either case, the driving force is less than those previously considered for electron transfer between the monophosphine-substituted ions $Mn(CO)_5L^+$ and $Mn(CO)_4P^-$ (where L and P represent various monophosphines).[52] The electron-transfer rates accompanying the annihilation of those ion pairs were immeasurably fast.[53] Even if the differences in the driving forces are taken into account, the electron-transfer rates for I^+ and II^- appear to be slower than those of the monosubstituted analogues. Inasmuch as both systems consist of carbonylmanganese ions of similar types, the ion-pair work terms and solvent reorganization energies in the Marcus context should be comparable.[54] In this light, the rather slow electron transfer between I^+ and II^- may reflect the rearrangement of trans to cis carbonyls and/or the increased inner-sphere reorganization energies derived from the pair of sterically encumbered DPPE ligands. The annihilation of the ion pair I^+/II^- by electron transfer in eq 16 can be observed directly by allowing a frozen mixture consisting of a layer of $I^+PF_6^-$ separated from a layer of $II^-NBu_4^+$ in acetonitrile to thaw (see Experimental Section). When the experiment was carried out in the cavity of the ESR spectrometer, a spectrum similar to that shown in Figure 2 was observed.

Experimental Section

Materials. Manganese decacarbonyl (Pressure Chemical Co.) was used as received. 1,2-Bis(diphenylphosphino)ethane (DPPE) from Pressure Chemical Co. was recrystallized from absolute ethanol and dried in vacuo at 0.1 mmHg. Tetra-*n*-butylammonium perchlorate (TBAP, Pfaltz and Bauer) was recrystallized three times from ethyl acetate–hexane, followed by drying in vacuo at 80 °C. The pure, dry salt was stored over P_2O_5 in a desiccator. Tetrahydrofuran (Fisher) was stirred with $LiAlH_4$ (Aldrich) for 24 h and fractionally distilled under an argon atmosphere. The distillate was stored under argon in a Schlenk flask equipped with Teflon stopcocks. Benzene (Fisher) was fractionally distilled from sodium–benzophenone and stored in a Schlenk flask under an argon atmosphere. Hexane was similarly treated after distillation from Na–K alloy (50% w/w) under an argon atmosphere. Acetonitrile (Fisher) was stirred with solid $KMnO_4$ (excess) for 24 h and the mixture refluxed until extensive amounts of MnO_2 formed. Decantation was followed by treatment with P_2O_5 and a small amount of diethylenetriamine. After the clear solution was refluxed for 5 h, it was fractionated under an argon atmosphere and stored in Schlenk flasks.

Instrumentation. Infrared spectra were recorded on a Nicolet 10DX FT spectrometer with 0.1-mm NaCl cells. ^1H and ^{31}P NMR spectra were obtained on a JEOL FX90Q or Nicolet NT300-WB spectrometer with chemical shifts reported relative to TMS and H_3PO_4, respectively. ESR spectra were recorded on a Varian E110 spectrometer with a DPPH lock. All manipulations of the air-sensitive carbonylmanganese compounds were carried out in a Vacuum Atmospheres MO-41 box. The conventional cyclic voltammetry at $v < 100\ V\ s^{-1}$ and preparative-scale electrolysis were carried out as described previously.[2,17] Fast-scan cyclic voltammetry at $v > 200\ V\ s^{-1}$ employed 10-μm Pt wire (Goodfellows, London) sealed in soft glass and polished to a mirror finish. Electrode connections were made with conductive paint (Nickel Print, GE Electronics). The three-electrode potentiostat was constructed locally and employed fast-response Motorola LF-357 operational amplifiers.[55] The voltage-follower circuit was mounted external to the potentiostat to minimize the length of the wire from the working electrode and thus ensure low noise pickup. The potentiostat was driven by a Princeton Applied Research Model 175 universal programmer or Exact Model 628 function generator. Current and voltage signals were transferred to a Gould Biomation 4500 digital oscilloscope with 8-bit resolution and 10-ns response time. The interface to a Compaq Deskpro PC Model 3 allowed all further data manipulation (including subtraction of the charging current). All fast-scan cyclic voltammograms were performed in a Faraday cage to minimize 60-Hz interference. Voltages are reported

(46) See: Amatore, C.; Gareil, M.; Saveant, J. M. *J. Electroanal. Chem. Interfacial Electrochem.* **1983**, *147*, 1 and references therein.
(47) McCullen, S. B.; Brown, T. L. *J. Am. Chem. Soc.* **1982**, *104*, 7496. See also ref 17.
(48) See also: (a) Walker, H. W.; Herrick, R. S.; Olsen, R. J.; Brown, T. L. *Inorg. Chem.* **1984**, *23*, 3748. (b) Caspar, V. J.; Meyer, T. J. *Chem. Rev.* **1985**, *85*, 187.
(49) For another recent example, see ref 32. See also: Fox, M. A.; Akaba, R. *J. Am. Chem. Soc.* **1983**, *105*, 3460.
(50) Based on $E^\circ_2 = -1.45$ V and $E^\circ_1 = -1.76$ V.
(51) From the Nernst equation with $E^\circ_2 = E^\circ_1 + 0.059 \log K$ at 25 °C.
(52) Lee, K. Y.; Kuchynka, D. J.; Kochi, J. K. *Organometallics* **1987**, *6*, 1886.
(53) Upon mixing solutions of the cations and anions.
(54) Assuming a Marcus theory outer-sphere electron transfer. See: Marcus, R. A. *J. Chem. Phys.* **1956**, *24*, 966; **1957**, *26*, 867; **1965**, *43*, 679.
(55) Howell, J. O.; Kuhr, W. G.; Ensman, R. E.; Wightman, R. M. *J. Electroanal. Chem. Interfacial Electrochem.* **1986**, *209*, 77.

relative to a saturated KCl–SCE reference electrode.

Preparation of *trans*-$Mn(CO)_2(DPPE)_2^+$. Dimanganese decacarbonyl (0.5 g, 1.3 mmol) and DPPE (1.02 g, 2.56 mmol) were dissolved in 25 mL of benzene, and the solution was refluxed for 4 h. The orange-yellow solid was collected, and a small amount dissolved in THF revealed a pair of bands at 1898 and 1865 cm^{-1} in the IR spectrum. Spectral subtraction of the carbonyl bands of an authentic sample of $NaMn(CO)_5$ prepared via sodium amalgam reduction of $Mn_2(CO)_{10}$[6] revealed a single sharp band at 1897 cm^{-1}, previously attributed to *trans*-$Mn(CO)_2(\eta^2\text{-DPPE})_2^+$;[4] yield of $I^+Mn(CO)_5^-$ 1.03 g (73%). A sample of $I^+Mn(CO)_5^-$ was dissolved in acetonitrile, and 1 equiv of $Cp_2Fe^+PF_6^-$ was added. After 15 min, the $Mn(CO)_5^-$ moiety was replaced by $Mn_2(CO)_{10}$ as judged from an inspection of the IR spectrum. Addition of diethyl ether yielded $I^+PF_6^-$, which upon recrystallization from dichloromethane–hexane afforded the crystalline, air-stable salt (ν_{CO} = 1897 cm^{-1} in CH_2Cl_2). The perchlorate salt was prepared by the addition of 1 equiv of anhydrous $AgClO_4$ to a solution of $I^+Mn(CO)_5^-$ in acetonitrile. After the mixture was stirred for 10 min, the black precipitate of silver was removed and the IR spectrum revealed the presence of $I^+ClO_4^-$ (ν_{CO} = 1897 cm^{-1}), $Mn_2(CO)_{10}$, and an unidentified carbonyl-containing product with a single band at 1941 cm^{-1}. Filtration of the solution through a column of Celite (Aldrich) followed by addition of diethyl ether yielded the perchlorate salt. The chloride salt was obtained simply by the dissolution of $I^+Mn(CO)_5^-$ in chloroform to immediately form an orange-red solution. Filtration followed by precipitation with hexane afforded I^+Cl^-, which upon recrystallization from dichloromethane–hexane yielded golden yellow crystals of I^+Cl^-. The $^{31}P\{^1H\}$ NMR spectra of all four salts in $CDCl_3$ showed a single sharp resonance at δ 77.8, at both 25 and −60 °C. To confirm the identity of the salts of $Mn(CO)_2(DPPE)_2^+$, the bromide salt was prepared independently from 0.16 g (0.32 mmol) of $Mn(CO)_3(DPPE)Br$ and 0.20 g (0.38 mmol) of DPPE in 15 mL of MeOH after refluxing for 48 h.[17,56] Removal of MeOH in vacuo, followed by crystallization of the residue from dichloromethane, afforded I^+Br^-, whose spectral properties were identical with those of the salts above.

Preparation of $Mn(CO)_2(DPPE)(PPhMe_2)Br$. $Mn(CO)_3(DPPE)Br$ (0.1 g, 0.16 mmol) and $PPhMe_2$ (0.022 g, 0.16 mmol) were dissolved in 10 mL of benzene, and the solution was refluxed for 36 h. The IR spectrum of the solution revealed a pair of carbonyl bands with equal intensity at 1863 and 1938 cm^{-1} consistent with the *mer* isomer of $Mn(CO)_2L_2LBr$[25] as in $Mn(CO)_2(PPhMe_2)_3Br$ with ν_{CO} = 1851 and 1929 cm^{-1}. Removal of benzene in vacuo and crystallization from chloroform–hexane yielded $Mn(CO)_2(DPPE)(PPhMe_2)Br$. $^{31}P\{^1H\}$ NMR ($CDCl_3$, −60 °C): δ 79.5 (d of d, 63.5 and 22.0 Hz), 55.2 (d of d, 44.0 and 22.0 Hz), and 23.4 (d of d, 63.5 and 44.0 Hz). Due to slow decomposition in both the solid and solution phases, we have been unable to attain analytically pure samples for elemental analysis.

Synthesis of $Mn(CO)_2[P(OMe)_3]_4^+BF_4^-$. A solution of *fac*-$Mn(CO)_3(NCMe)_3^+BF_4^-$[3] in acetonitrile was refluxed with excess trimethyl phosphite for 12 h. Removal of the solvent in vacuo followed by recrystallization from dichloromethane–hexane afforded *cis*-$Mn(CO)_2[P(OMe)_3]_4^+BF_4^-$.[57]

Cyclic Voltammetry. In a typical procedure, a thoroughly dried CV cell[2,17] was charged with 0.032 g (0.03 mmol) of $I^+PF_6^-$ and 6 mL of 0.3 M TBAP in THF under an argon atmosphere. The initial negative-scan cyclic voltammograms (Figures 1 and 4) were obtained with a Pt electrode at various scan rates (e.g., see Table I). No evidence for electrode pollution could be discerned, and repetitive cyclic voltammograms were reproducible over a period of several hours. The cyclic voltammetry in acetonitrile containing 0.1 M TBAP was similar to that in THF except that wave A was shifted to −1.97 V and wave B to −1.25 V with $E_{1/2}$ = −1.40 V (ΔE_p = 200 mV). No curve crossing was observed. For the fast-scan cyclic voltammetry, the Pt macroelectrode was simply replaced by the microelectrode and the experiment was otherwise carried out in the conventional manner. Peak potentials and peak currents were calibrated by comparison with those of a ferrocene standard.[29] The initial positive-scan CV of I^+ was examined earlier.[9] It showed a reversible 1e couple at $E_{1/2}$ = 0.98 V with i_p^c/i_p^a = 1.0 and ΔE_p = 83 mV at v = 500 mV s^{-1}. The ESR spectrum of I^{2+} consisted of a_{Mn} = 93 G with no resolvable ^{31}P splitting.

Electrolytic and Chemical Preparation of $Mn(CO)_2(DPPE)_2^-$ (II^-). A thoroughly dried three-compartment electrolysis cell was charged under an argon atmosphere (glovebox) with 0.30 g (0.28 mmol) of $I^+PF_6^-$ and 28 mL of a 0.5 M solution of TBAP in THF. The working and reference compartments were also filled with the 0.5 M TBAP solution in THF. The controlled-potential reduction of the golden yellow solution was carried out at −2.0 V until the current fell to the background level and the solution had become very dark red. Coulometry indicated that 52.7 C was passed, which corresponded to an uptake of 1.95 equiv of charge per mole of $Mn(CO)_2(DPPE)_2^+$ initially present. IR analysis of the catholyte revealed four sharp bands in the carbonyl region at 1710 and 1766 cm^{-1} for $Mn(CO)_2(DPPE)_2^-$ and at 1856 and 1915 cm^{-1} for $HMn(CO)_2(DPPE)_2$ (vide infra). CV analysis of the catholyte showed an anodic wave with a reversible couple at $E_{1/2}$ = −1.45 V for $Mn(CO)_2(DPPE)_2^-$. The irreversible cathodic wave of $Mn(CO)_2(DPPE)_2^+$ at E_p^c = −1.84 V (0.5 V s^{-1}, vide supra) was absent. The yield of $Mn(CO)_2(DPPE)_2^-$ was estimated to be ~40% on the basis of the intensity of the carbonyl bands in the IR spectrum and the magnitude of the anodic peak current in the cyclic voltammogram. No significant increase in the yield of II^- was realized when the same bulk electrolysis was carried out at −25 °C. However, when the reduction was carried out in acetonitrile solution (containing 0.1 M TBAP), 2.02 equiv of charge was taken up at a constant potential of −2.20 V. The resulting deep red solution also contained a precipitate. CV analysis of the catholyte showed a reversible anodic wave of $Mn(CO)_2(DPPE)_2^-$ at $E_{1/2}$ = −1.40 V and no cathodic wave of I^+. IR analysis of the catholyte again revealed four sharp bands in the carbonyl region at 1706 and 1761 cm^{-1} for $Mn(CO)_2(DPPE)_2^-$ and at 1844 and 1909 cm^{-1} for $HMn(CO)_2(DPPE)_2$.[8] An estimated yield of 70% for $Mn(CO)_2(DPPE)_2^-$ was ascertained for the anodic peak current in the CV analysis. No substantial improvement in the yield of II^- was noted when the experiment was repeated at −30 °C.

Various attempts were made to prepare $Mn(CO)_2(DPPE)_2^-$ with different reducing agents as follows. Under an argon atmosphere, $I^+PF_6^-$ (0.3 g) was treated with Na–K (0.1 mL of a 50% w/w alloy amalgamated with 1 mL of Hg) in THF to yield a dark red solution within 10 min. IR and CV analysis indicated high yields of $Mn(CO)_2(DPPE)_2^-$. (Furthermore, the addition of CO led to high yields of $Mn(CO)_3(DPPE)^-$ (vide supra).) However, all attempts to isolate the salt led to only $HMn(CO)_2(DPPE)_2$.[8] Apparently traces of protic impurities effectively converted II^- to III. When unamalgamated Na–K alloy was employed, overreduction occurred and no carbonyl-containing product was detected. The use of sodium naphthalenide in THF as the reductant led to a mixture of II^- and III. The reduction of $I^+PF_6^-$ with 1% sodium amalgam in THF led to high yields of $HMn(CO)_2(DPPE)_2$.

Deprotonation of $HMn(CO)_2(DPPE)_2$ in THF with excess *n*-butyllithium at −45 °C resulted in a dark red solution. CV analysis following the addition of 0.3 M $LiClO_4$ indicated the presence of $Mn(CO)_2(DPPE)_2^-$ as judged by the reversible wave at $E_{1/2}$ = −1.40 V. A second irreversible anodic wave was observed at E_p^a = −0.41 V. The slight shifts in the potentials of $Mn(CO)_2(DPPE)_2^-$ and $Mn(CO)_2(DPPE)_2^\bullet$ in these experiments doubtlessly arose from the presence of lithium and hexane introduced with butyllithium.

The cyclic voltammetry of $HMn(CO)_2(DPPE)_2$ in THF solution containing 0.3 M TBAP showed only a single irreversible cathodic wave at −2.60 V with v = 0.5 V s^{-1}.

Electrosynthesis of $Mn(CO)_2[P(OMe)_3]_3^-$. The CV analysis of a 5×10^{-3} M solution of $Mn(CO)_2[P(OMe)_3]_4^+BF_4^-$ (IV^+) in THF containing 0.3 M TBAP revealed an irreversible 2e wave at E_p^c = −2.15 V at v = 0.5 V s^{-1}. Upon scan reversal, a quasi-reversible anodic wave at E_p^a = −0.98 V was observed with $E_{1/2}$ = −1.05 V and ΔE_p = 142 mV together with an irreversible anodic wave at E_p^a = −0.35 V. The cyclic voltammogram in acetonitrile containing 0.1 M TBAP was the same, except for slight (<30 mV) shifts in the potentials (vide supra). In this regard, the behavior of IV^+ is akin to that of I^+. The cyclic voltammograms of IV^+ in both THF and MeCN, however, showed no curve crossing. The initial CV wave of IV^+ remained irreversible up to v = 200 000 V s^{-1} in acetonitrile containing 0.2 M TBAP.

Constant-potential electrolysis of $IV^+BF_4^-$ in THF at −2.2 V resulted in an uptake of 2.03 equiv of charge/mol of IV^+, and the colorless solution turned golden yellow. No gas evolution was observed, but the distinctive odor of $P(OMe)_3$ was prevalent. CV analysis of the catholyte revealed that no $Mn(CO)_2[P(OMe)_3]_4^+$ was present, the predominant species being $Mn(CO)_2[P(OMe)_3]_3^-$ with $E_{1/2}$ = −1.05 V. IR analysis in THF indicated only a pair of carbonyl bands at 1821 and 1757 cm^{-1}. Treatment with acetic acid gave $HMn(CO)_2[P(OMe)_3]_3$ with carbonyl bands at 1949 and 1885 cm^{-1} as reported earlier by Berke and coworkers[19] for the *mer* isomer. The ^1H NMR spectrum of $HMn(CO)_2[P(OMe)_3]_3$ showed a distinctive Mn–H resonance at δ −7.50 (d of t, J_{PH} = 60 and 50 Hz) and a methyl resonance at δ 3.55 (br m). The $^{31}P\{^1H\}$ NMR spectrum consisted of a very broad resonance at δ 197 with $\Delta\nu_{1/2}$ = 230 Hz, which was partially resolved at −60 °C into a complex multiplet strongly indicative of second-order effects.

Electrochemical Preparation of $Mn(CO)_2(DPPE)(PPhMe_2)^-$. The 2e reductions of the various bromomanganese carbonyls $BrMn(CO)_{5-x}L_x$

(56) Colton, R.; McCormick, M. J. *Aust. J. Chem.* **1976**, *29*, 1657.
(57) (a) Uson, R.; Riera, V.; Gimeno, J.; Laguna, M.; Gamasa, M. P. *J. Chem. Soc., Dalton Trans.* **1979**, 996. (b) Reimann, R. H.; Singleton, E. *J. Chem. Soc., Dalton Trans.* **1974**, 808.

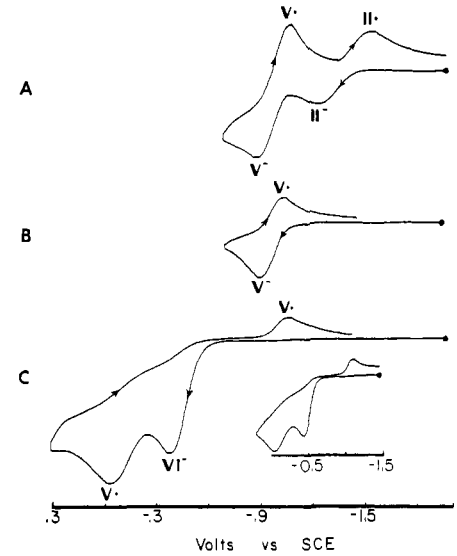

Figure 7. Cyclic voltammograms of 3×10^{-3} M $Mn(CO)_2(DPPE)_2^-$ (II^-) in THF containing 0.3 M TBAP at $v = 500$ mV s^{-1} under 1 atm of CO after (A) 1 min, (B) 10 min, and (C) 30 min. Inset: CV of $Mn(CO)_3(DPPE)^-$ (IV^-) under 1 atm of CO after 30 min. See text for discussion.

(where $x = 0$–4, L = phosphine) are known to yield the anionic $Mn(CO)_{5-x}L_x^-$ species with the expulsion of bromide (compare eq 9).[17,18] Accordingly, when $BrMn(CO)_2(DPPE)PPhMe_2$[25] was subjected to CV analysis in THF containing 0.3 M TBAP, an irreversible 2e cathodic wave was observed at −2.45 V. Upon scan reversal, a pair of anodic waves were observed at $E_p^a = -1.44$ and −0.55 V. The former showed quasi-reversible behavior and was assigned to $Mn(CO)_2(DPPE)(PPhMe_2)^-$ on the basis of its electrochemical parameters with $E_{1/2} = -1.50$ V, $i_p^c/i_p^a = 1.0$, and $\Delta E_p = 165$ mV at 0.5 V s^{-1}. The second irreversible wave was ascribed to the further oxidation of the radical.[58]

Carbonylation of $Mn(CO)_2(DPPE)_2^-$. When a THF solution of $Mn(CO)_2(DPPE)_2^-$ (prepared electrolytically as described above) was exposed to 1 atm of carbon monoxide, the dark red solution changed to orange as rapidly as gaseous diffusion allowed. IR analysis of the resulting solution showed carbonyl bands at 1867, 1784, and 1772 cm^{-1}, which were identical with those of an authentic sample of $Mn(CO)_3(DPPE)^-NBu_4^+$ ($V^-NBu_4^+$).[17] The latter was confirmed by CV analysis showing the reversible $Mn(CO)_3(DPPE)^-/Mn(CO)_3(DPPE)^\bullet$ couple with $E_{1/2} = -1.05$ V vs SCE.[17] When it stood for ~30 min under a continued CO atmosphere, $Mn(CO)_3(DPPE)^-$ was converted to another species with carbonyl bands at 1942, 1853, 1822, and 1772 cm^{-1}, which was assigned to the monodentate derivative $Mn(CO)_4(\eta^1\text{-DPPE})^-$ owing to the close similarity of this IR spectrum to that of $Mn(CO)_4PPh_3^-$ with $\nu_{CO} = 1945$, 1854, 1827, and 1777 cm^{-1}.[6,52] The same result was obtained when an authentic sample of $Mn(CO)_3(DPPE)^-NBu_4^+$ was exposed to 1 atm of CO for 30 min.

The rapidity with which $Mn(CO)_2(DPPE)_2^-$ (II^-) undergoes carbonylation in eq 10 is illustrated by the sequence of cyclic voltammograms in Figure 7. The initial positive-scan CV in Figure 7A taken 1 min after the introduction of CO shows the reversible CVs of both $II^-/II^\bullet$ and $V^-/V^\bullet$ at $E_{1/2} = -1.45$ and −1.05 V, respectively. After 10 min (Figure 7B) the $II^-/II^\bullet$ couple has disappeared completely with only the $V^-/V^\bullet$ couple present, as described in eq 10. The second carbonylation, i.e.

$$\underset{V^-}{Mn(CO)_3(DPPE)^-} + CO \rightarrow \underset{VI^-}{Mn(CO)_4(\eta^1\text{-DPPE})^-} \qquad (17)$$

then occurs in a subsequent slower step. Thus after 30 min (Figure 7C), a pair of irreversible anodic waves are observed with $E_p^a = -0.44$ and −0.10 V that upon scan reversal show the cathodic wave corresponding to $V^\bullet \xrightarrow{e^-} V^-$. The inset in Figure 7 is the cyclic voltammogram of an authentic sample of $Mn(CO)_3(DPPE)^-$ after exposure to CO for 30 min. Thus, the irreversible CV wave at −0.44 V is ascribed to the oxidation of $Mn(CO)_4(\eta^1\text{-DPPE})^-$ (VI^-) since it compares with $E_p^a = -0.50$ V for $Mn(CO)_4PPh_3^-$.[2] The resulting 17e radical $VI^\bullet$ undergoes a facile rearrangement to regenerate $V^\bullet$ by CO expulsion, i.e.

$$\underset{VI^\bullet}{Mn(CO)_4(\eta^1\text{-DPPE})^\bullet} \rightarrow \underset{V^\bullet}{Mn(CO)_3(\eta^2\text{-DPPE})^\bullet} + CO \qquad (18)$$

as seen by the cathodic wave at −1.11 V. The irreversible anodic wave at $E_p^a = -0.10$ V is associated with the further oxidation of $V^\bullet$, i.e.[59]

$$\underset{V^\bullet}{Mn(CO)_3(\eta^2\text{-DPPE})^\bullet} \xrightarrow{-e^-} \underset{V^+}{Mn(CO)_3(\eta^2\text{-DPPE})^+}, \text{ etc.}$$

The rapid rate of CO expulsion in eq 18 further underscores the substitution lability of 17e radicals even in competition with (second-order) dimerization rates near the diffusion-controlled limit.[28]

Finally, the CV studies of $Mn(CO)_2(DPPE)_2^+$ also illustrate the rapidly with which the anionic $Mn(CO)_2(DPPE)_2^-$ undergoes carbonylation. Thus, an initial negative-scan CV at 0.5 V s^{-1} shows the irreversible cathodic wave of I^+ slightly shifted to negative potentials ($E_p^c = -1.92$ V), but upon scan reversal no curve crossing was observed. Only the reversible oxidation of $Mn(CO)_3(DPPE)^-$ at $E_{1/2} = -1.05$ V was apparent with no trace of the $II^-/II^\bullet$ couple at $E_{1/2} = -1.45$ V.

ESR Spectrum of $Mn(CO)_2(\eta^2\text{-DPPE})(\eta^1\text{-DPPE})$. Two procedures were used to generate $II^\bullet$ for the ESR studies. In the first method, 28 mL of a 5×10^{-3} M solution of I^+ containing 0.3 M TBAP in tetrahydrofuran was initially reduced to II^- as described above. The solution was then reoxidized potentiostatically at −1.0 V until the current flow ceased (uptake of ~0.8 e/II^-). Immediately thereafter 0.3 mL of anolyte was transferred under an argon atmosphere to a quartz ESR tube. The solution was frozen and degassed, and the contents were sealed in vacuo. The frozen mixture was allowed to warm up in the cavity of the ESR spectrometer. Alternatively, 0.3 mL of a 5×10^{-3} M solution of I^+ in THF was added to an ESR tube and frozen. To this mixture was added a solution of II^- (vide supra), and the entire contents were refrozen. The tube was sealed in vacuo and allowed to warm up in the cavity of the ESR spectrometer. The same ESR spectrum (Figure 2A) was obtained by both procedures and by carrying out analogous studies in acetonitrile. Attempts to improve the resolution of the ESR spectrum included the selective saturation of a putative second signal (that may have given rise to what appeared to be a broad singlet with $\Delta H_{pp} \approx 100$ G) by increasing the microwave power from 0.5 to 20 or 30 mW. Changes in the modulation amplitude also had an effect on the resolution. The ESR spectrum in THF at 77 K revealed a complex anisotropic spectrum, which was not fully characterized.

The computer simulation of the ESR spectrum in Figure 2B was based on $a_{2P} = 20$ G, $a_P = 42$ G, a_P 17 G, and $a_{Mn} = 9$ G, having Lorentzian line shapes with $\Delta H_{pp} = 12$ G, with use of the computer program ESRSIM-FTN kindly provided by Dr. R. Sustmann (University of Essen). Other combinations of ^{31}P hfs also gave the general splitting pattern of the experimental spectrum in Figure 2A. For example, $a_{2P} = 21$ G, $a_P = 42$ G, and $a_{Mn} = 5$ G added to a 120-G singlet with an intensity ratio 1:0.4, respectively, provided a reasonable simulation but the outermost wing lines of the simulated spectrum were severely broadened to a point of being barely discernible. Owing to the broad lines in the experimental spectrum, we were unable to provide any further improvements for unambiguous fits to the experimental spectrum.

Digital Simulation of the Cyclic Voltammograms. The computer simulation of the redox chemistry of $Mn(CO)_2(DPPE)_2^+$ was carried out by the finite difference approach of Feldberg.[43,44] The simulation of a full-cycle voltammogram consisted of 1000 discrete data points to allow for the acceptable resolution of the experimental cyclic voltammograms. The kinetics for the formation of $II^\bullet$ from the conversion of $I^\bullet$ via reduction of I^+ was assumed to be a first-order process, i.e. $d[II^\bullet]/dt = k_r[I^\bullet]$. Since the experimental value of k_r was determined to have a minimum value of $\sim 4 \times 10^6$ s^{-1}, the disproportionation process was simplified to

$$I^+ + II^- \underset{k_d}{\overset{k_a}{\rightleftharpoons}} 2II^\bullet$$

and the rate processes were taken as

$$d[II^\bullet]/dt = k_{et}[I^+][II^-]$$

$$-d[I^+]/dt = -d[II^-]/dt = k_d[II^\bullet]^2$$

Inclusion of the heterogeneous electron-transfer kinetics thus determined defined the concentration of all species at any given distance from the electrode.[44b]

Acknowledgment. We gratefully acknowledge financial support from the National Science Foundation and the Robert A. Welch Foundation. J.K.K. thanks the Alexander von Humboldt Foundation and Professor R. W. Hoffmann and his colleagues for their kind hospitality during his stay at Fachbereich Chemie, Philipps Universität Marburg, at which this article was written.

(58) For other examples of such processes, see ref 17.

(59) The coordinatively unsaturated cation V^+ is subject to rapid solvation; see ref 2 and 17.